Electronic Supplementary Material (ESI) for New Journal of Chemistry.


# Supporting Informatin

## White-light-emitting lanthanide metal-organic framework for luminescent turn-off sensing of $MnO_4^-$ and turn-on sensing of folic acid and construction of “turn-on plus” system

*Zhen-Peng Dong, Fei Zhao, Zhi-Liang Liu and Yan-Qin Wang**

**Table S1.** Main Bond lengths (Å) and main bond angles (°) of Eu-MOF-**1**.

| | | | |
|---|---|---|---|
| Bond lengths (Å) | | | |
| Eu1-O2A | 2.328(9) | Eu1-O6C | 2.379(8) |
| Eu1-O8A | 2.331(9) | Eu1-O5B | 2.388(8) |
| Eu1-O1 | 2.393(9) | Eu1-O7 | 2.422(9) |
| Eu1-O10 | 2.451(13) | Eu1-O9 | 2.551(11) |
| Bond angles (°) | | | |
| O2A-Eu1-O8A | 73.0(3) | O2A-Eu1-O6C | 147.6(4) |
| O8A-Eu1-O6C | 137.9(3) | O2A-Eu1-O5B | 84.2(3) |
| O8A-Eu1-O5B | 81.7(3) | O6C-Eu1-O5B | 90.7(3) |
| O2A-Eu1-O1 | 121.4(3) | O8A-Eu1-O1 | 78.2(3) |
| O6C-Eu1-O1 | 81.9(3) | O5B-Eu1-O1 | 139.9(3) |
| O2A-Eu1-O7 | 80.4(3) | O8A-Eu1-O7 | 121.7(3) |
| O6C-Eu1-O7 | 86.4(3) | O5B-Eu1-O7 | 145.9(4) |
| O1-Eu1-O7 | 73.2(3) | O2A-Eu1-O10 | 76.9(4) |
| O8A-Eu1-O10 | 143.0(4) | O6C-Eu1-O10 | 70.9(4) |
| O5B-Eu1-O10 | 74.2(4) | O1-Eu1-O10 | 137.3(4) |
| O7-Eu1-O10 | 72.8(4) | O2A-Eu1-O9 | 137.0(3) |
| O8A-Eu1-O9 | 69.2(3) | O6C-Eu1-O9 | 69.2(4) |
| O5B-Eu1-O9 | 70.7(3) | O1-Eu1-O9 | 69.8(3) |
| O7-Eu1-O9 | 137.9(3) | O10-Eu1-O9 | 125.4(4) |

Symmetry transformations used to generate equivalent atoms: A: -x+1, -y+1, -z+1; B: -x+2, -y+1, -z; C: x, y, z+1.

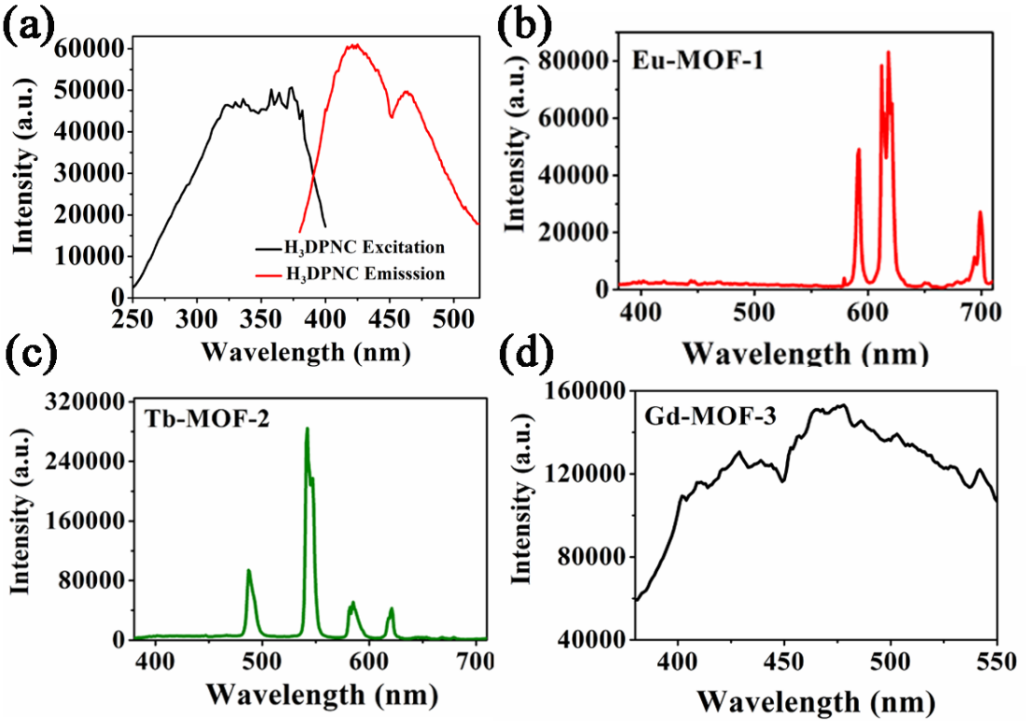


**Fig. S1.** The solid-state excitation and emission spectra of $H_3DPNC$ ligand and MOFs **1–3** at room temperature.

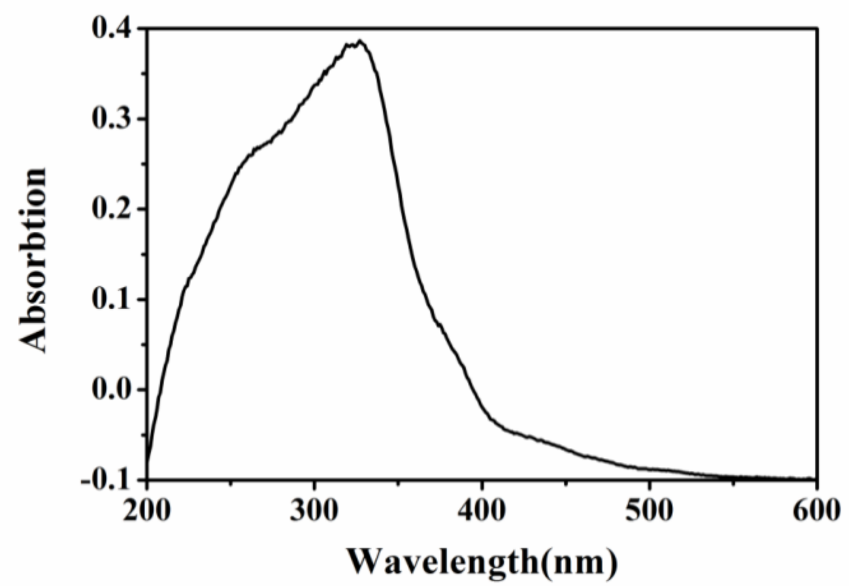


**Fig. S2.** The solid UV-vis absorption spectrum of $H_3DPNC$ ligand.

**Table S2**. Mixed metal Ln-MOFs $Eu_xTb_yGd_{1-x-y}$-DPNC with different molar ratios.

| Number | x | y | 1-x-y |
|---|---|---|---|
| 1 | 0.08 | 0.02 | 0.90 |
| 2 | 0.07 | 0.03 | 0.90 |
| 3 | 0.06 | 0.04 | 0.90 |
| 4 | 0.08 | 0.04 | 0.88 |
| 5 | 0.07 | 0.05 | 0.88 |
| 6 | 0.08 | 0.07 | 0.85 |
| 7 | 0.12 | 0.08 | 0.80 |
| 8 | 0.11 | 0.09 | 0.80 |
| 9 | 0.15 | 0.10 | 0.75 |
| 10 | 0.13 | 0.12 | 0.75 |
| 11 | 0.20 | 0.10 | 0.70 |
| 12 | 0.25 | 0.15 | 0.60 |
| 13 | 0.30 | 0.20 | 0.50 |
| 14 | 0.40 | 0.20 | 0.40 |
| 15 | 0.40 | 0.30 | 0.30 |
| 16 | 0.50 | 0.30 | 0.20 |

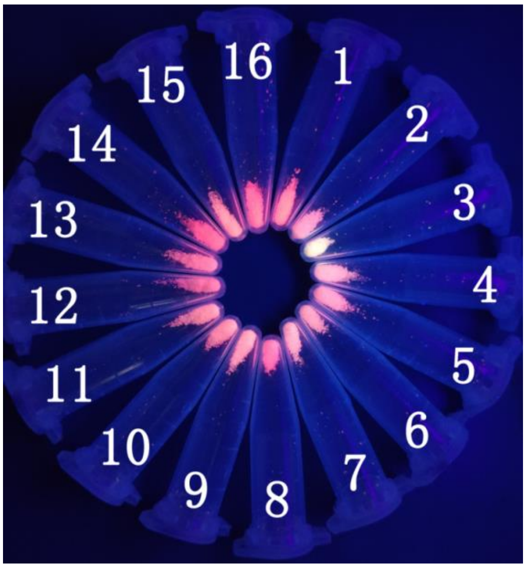


**Fig. S3.** Photographs of mixed metal Ln-MOFs $Eu_xTb_yGd_{1-x-y}$-DPNC with different molar ratios excited at 365 nm UV lamp.

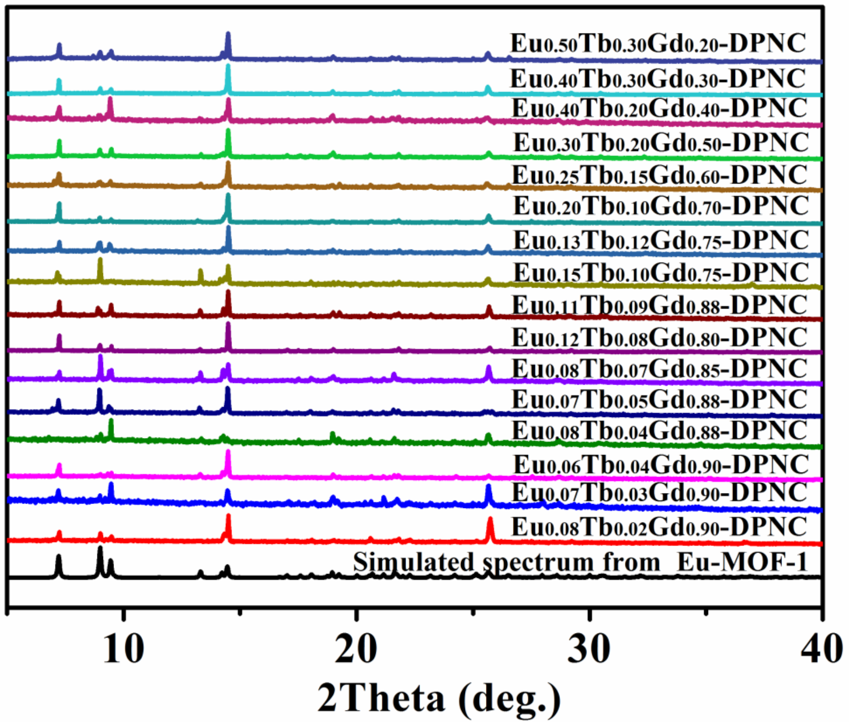


**Fig. S4.** PXRD patterns of mixed-Ln-MOFs $Eu_xTb_yGd_{1-x-y}$-DPNC with different the molar ratio.

**Table S3.** The molar ratios analysis of lanthanide ions by ICP for $Eu_{0.06}Tb_{0.04}Gd_{0.9}$–DPNC.

| MOF | Molar ratio of the reactant Eu/Tb/Gd salt | Eu/Tb/Gd mass ratio | Real Eu/Tb/Gd molar ratio |
|---|---|---|---|
| $Eu_{0.06}Tb_{0.04}Gd_{0.9}$-DPNC | 6:4:90 | 3.95: 2.52:57.23 | 5. 68:4.38:90.65 |

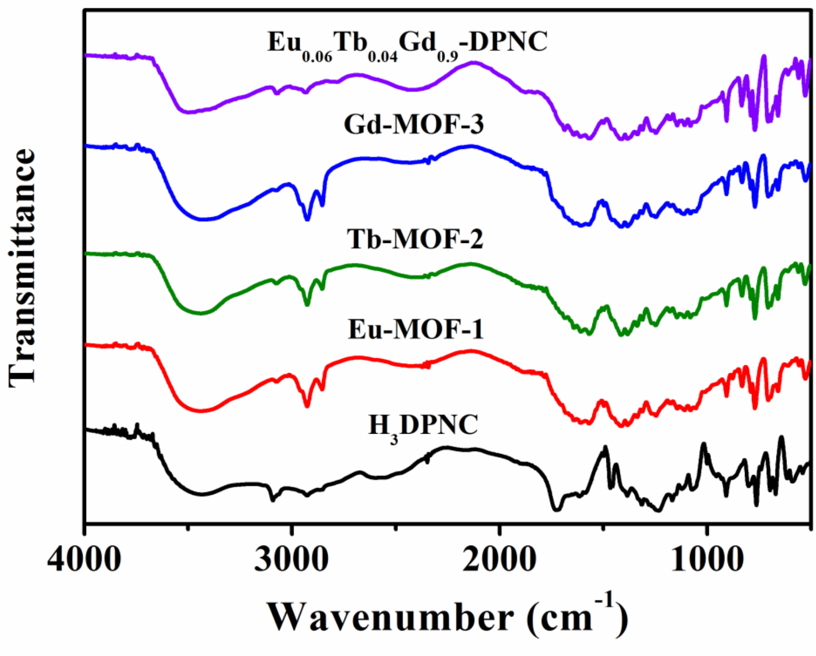


**Fig. S5.** FT-IR spectra of ligand and MOFs **1–4**.

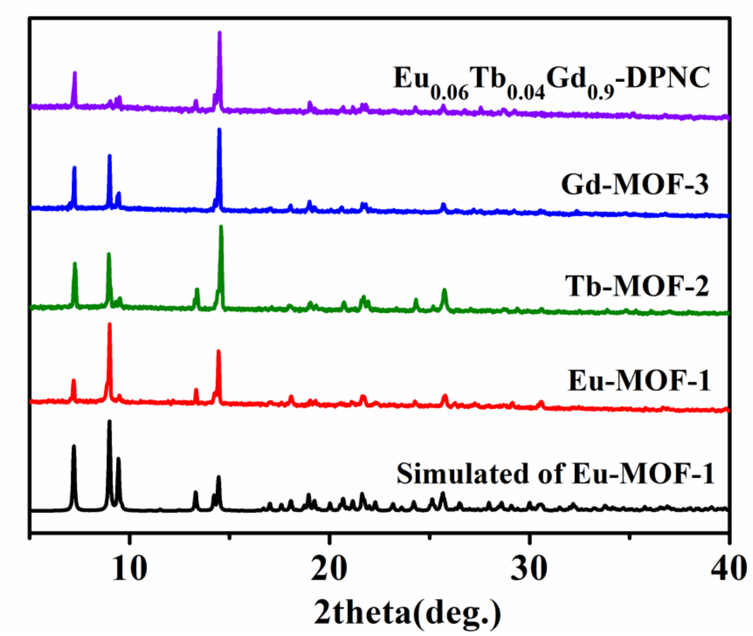


**Fig. S6.** PXRD patterns of simulated spectrum and MOFs **1–4**.

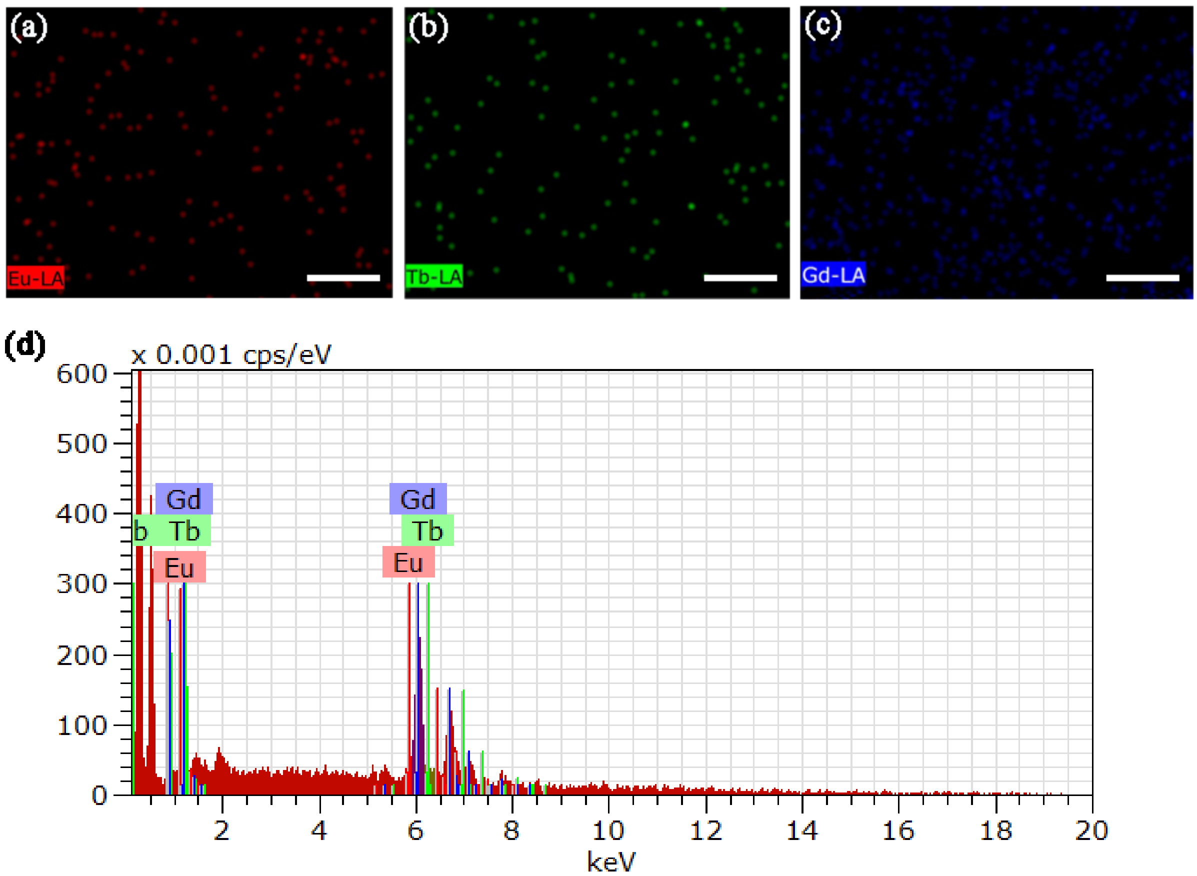


**Fig. S7.** (a, b, c) Elemental mapping images (red, green and blue dots represent the Eu, Tb and Gd elements, respectively) and (d) EDX−spectra of $Eu_{0.06}Tb_{0.04}Gd_{0.9}$−DPNC. Scale bar = 80 $\mu$m.

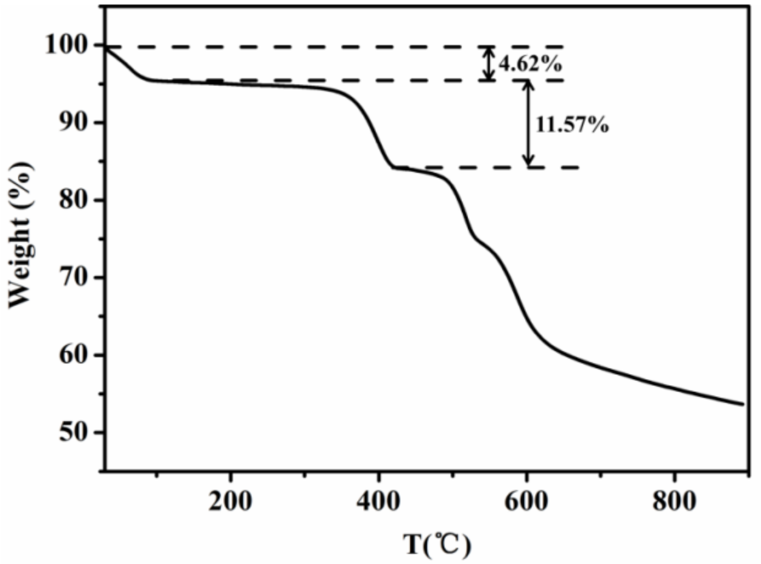


**Fig. S8.** TG curve of $Eu_{0.06}Tb_{0.04}Gd_{0.9}$–DPNC (MOF-**4**).

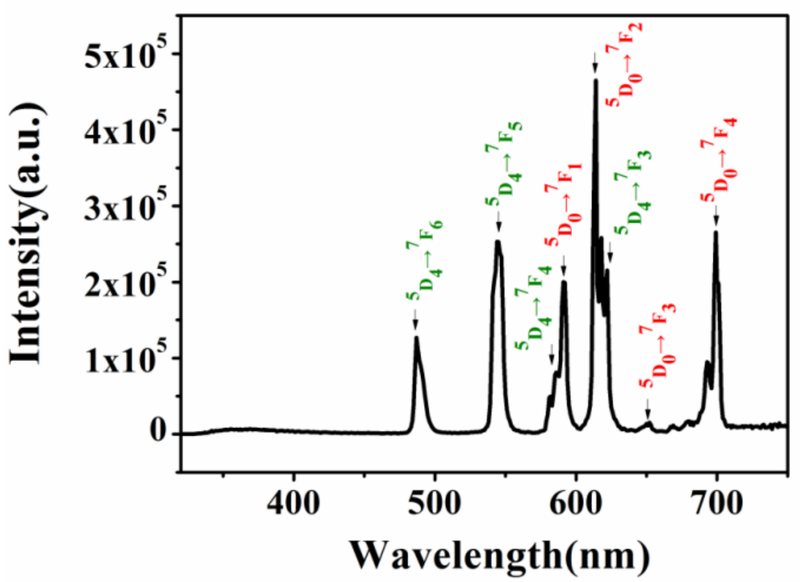


**Fig. S9.** The emission spectra of $Eu_{0.06}Tb_{0.04}Gd_{0.9}$–DPNC (MOF-**4**) excited at 320 nm.

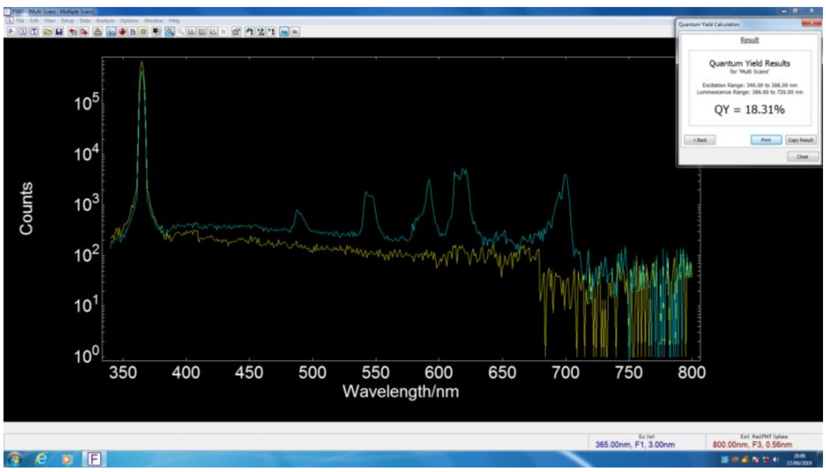


**Fig. S10.** The test data of absolute quantum yield of $Eu_{0.06}Tb_{0.04}Gd_{0.9}$–DPNC excited at 365 nm.

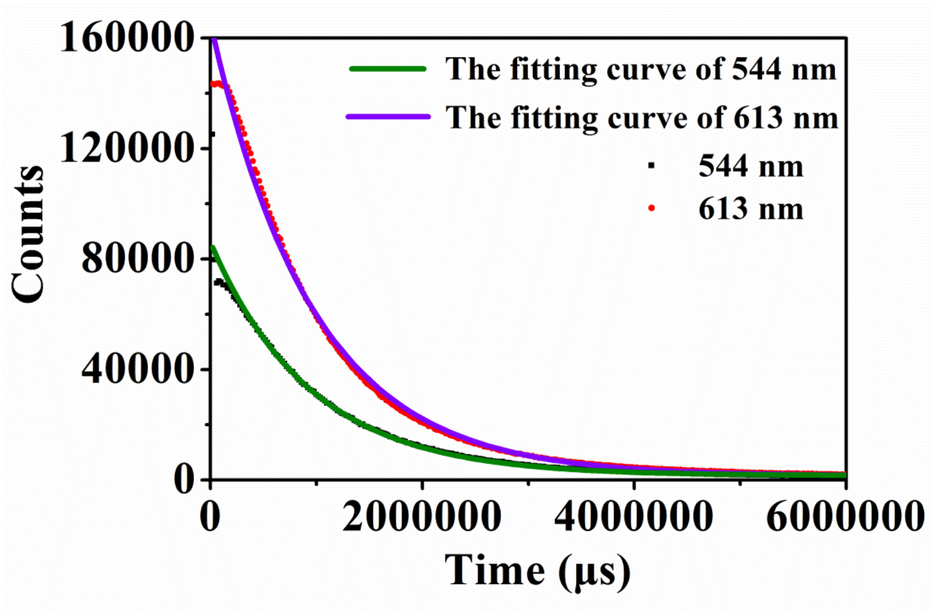


**Fig. S11.** The Fluorescence lifetime of $Eu_{0.06}Tb_{0.04}Gd_{0.9}$–DPNC with excitation under 365 nm.

**Table S4.** Luminescence lifetime and quantum yield (φ) of $Eu_{0.06}Tb_{0.04}Gd_{0.9}$–DPNC.

| MOF | τ (ms) | | quantum yield(φ) |
|---|---|---|---|
| | 544 nm | 613 nm | |
| $Eu_{0.06}Tb_{0.04}Gd_{0.9}$-DPNC | 0.95 | 0.98 | 18.31% |

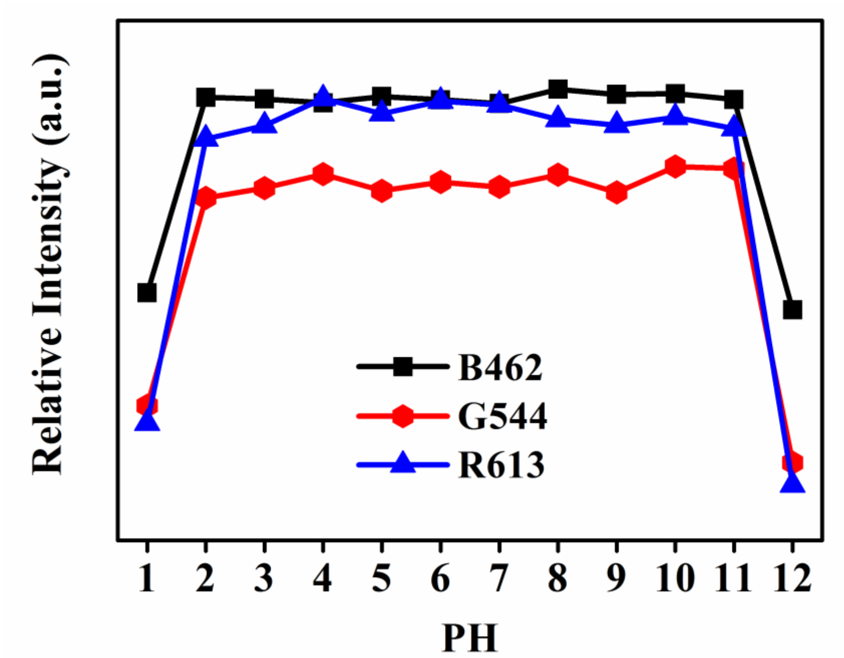


**Fig. S12.** Fluorescence measurements of $Eu_{0.06}Tb_{0.04}Gd_{0.9}$–DPNC after treatment with different pH aqueous solutions.

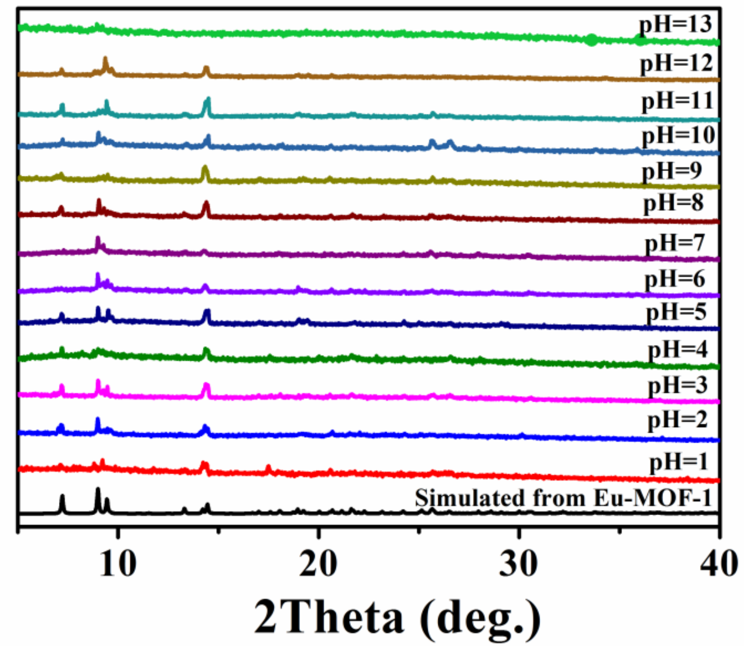


**Fig. S13.** PXRD patterns of $Eu_{0.06}Tb_{0.04}Gd_{0.9}$−DPNC after immersing in different pH aqueous solutions for 4 hours

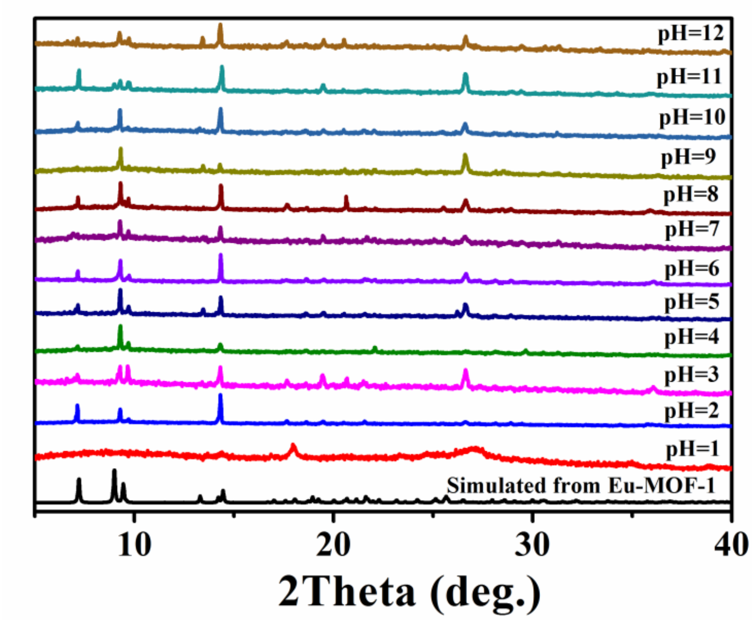


**Fig. S14.** PXRD patterns of $Eu_{0.06}Tb_{0.04}Gd_{0.9}$−DPNC after immersing in different pH aqueous solutions for 3 days.

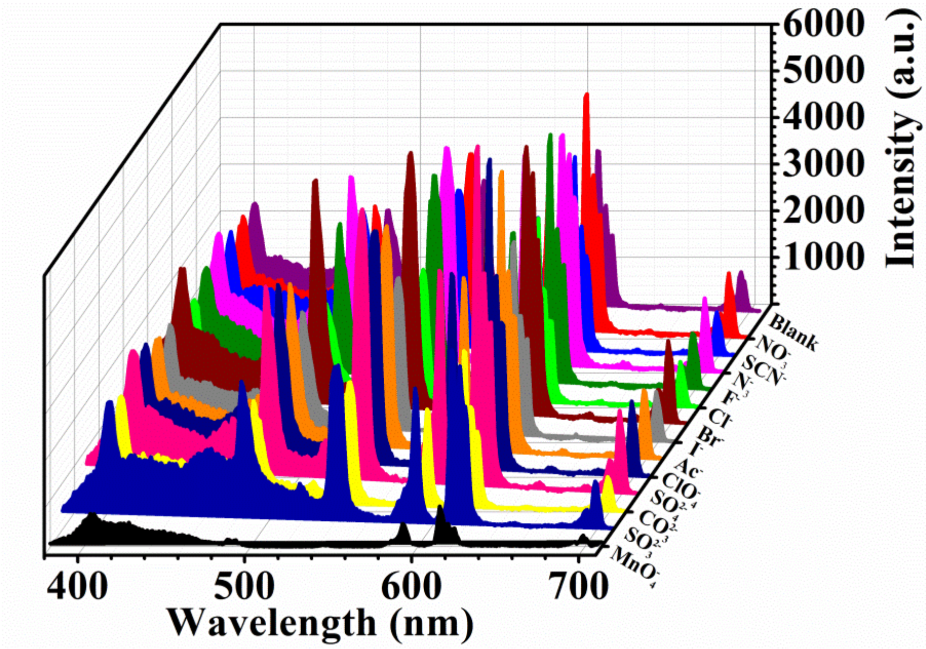


**Fig. S15.** Fluorescence response of $Eu_{0.06}Tb_{0.04}Gd_{0.9}$–DPNC in different anions aqueous solution.

**Table S5.** Standard deviation and limit of detection calculation for $Eu_{0.06}Tb_{0.04}Gd_{0.9}$–DPNC toward $MnO_4^-$.

| **No.** | Luminescence Intensity ($I_{544}$) of $Eu_{0.06}Tb_{0.04}Gd_{0.9}$–DPNC in $H_2O$ | Luminescence Intensity ($I_{613}$) of $Eu_{0.06}Tb_{0.04}Gd_{0.9}$–DPNC in $H_2O$ | $I_{616}$ /$I_{544}$ |
|---|---|---|---|
| 1 | 2927 a.u. | 3709 a.u. | 1.26717 |
| 2 | 3040 a.u. | 3752 a.u. | 1.23421 |
| 3 | 2978 a.u. | 3756 a.u. | 1.26125 |
| 4 | 2989 a.u. | 3731 a.u. | 1.24824 |
| 5 | 3038 a.u. | 3802 a.u. | 1.25148 |
| Standard Deviation (σ) | -- | -- | 0.01270 |
| Slope (S) | -- | -- | 1.93589 |
| Detection Limit (3σ/S) | -- | -- | 0.0197 |

**Table S6.** A summary of the MOFs for the sensing of $MnO_4^-$.

| No. | Molecular Formula | LOD /μM | Ref |
|---|---|---|---|
| 1 | $[Zn_2(BDC)_{1.5}(L_1)(DMF)]\cdot 1.5DMF$ | 0.03 | [1] |
| 2 | In-MOF-Eu | 147 | [2] |
| 3 | $[Co(NPDC)(bpee)]\cdot DMF\cdot 2H_2O$ | 1.5 | [3] |
| 4 | $[Tb(TBOT)(H_2O)](H_2O)_4(DMF)(NMP)_{0.5}$ | 340 | [4] |
| 5 | $[Co(L_2)(1,4\text{-}ndc)\cdot H_2O]_n$ | 0.014 | [5] |
| 6 | $[Co_2(L_3)(1,4\text{-}chdc)_2]_n$ | 0.012 | [5] |
| 7 | $[Zn(2,2'\text{-}bipy)(ppa)(H_2O)_2]\cdot 2H_2O$ | 6.73 | [6] |
| 8 | $[Tb(TATAB)(H_2O)]\cdot 2H_2O$ | 0.044 | [7] |
| 9 | $Eu_{0.06}Tb_{0.04}Gd_{0.9}$-DPNC | 0.0197 | This work |

$L_1$ = pyridine 4-carboxylic acid, BDC= benzene-1,4-dicarboxylate; NPDC = 2-nitro phenylenedicarboxylate, bpee = 1,2-bis(4-bipyridyl) Ethylene; $L_2$ = 1,1'-(1,4-butanediyl) bis(5,6-dimethylbenzimidazole), 1,4-ndc = 1,4-naphtha-lenedicarboxylic acid, $L_3$ = 1,1'-(1,4-butanediyl)bis(2-methylbenzimidazole), 1,4-chdc = 1,4-cyclohexanedioic acid; 2,2'-bipy = 2,2'-bipyridine, ppa = 3-(pyridiium-3-yloxy)phthalic acid; $H_3$TATAB = 4,4',4''-s-triazine-1,3,5-triyltri-m-amino-benzoic acid.

**Table S7.** Standard deviation and limit of detection calculation for $Eu_{0.06}Tb_{0.04}Gd_{0.9}$–DPNC toward FA.

| No. | Luminescence Intensity ($I_{462}$) of $Eu_{0.06}Tb_{0.04}Gd_{0.9}$–DPNC in $H_2O$ | $I/I_0$ |
|---|---|---|
| 1 | 4668 a.u. | 1 |
| 2 | 4717 a.u. | 1.01050 |
| 3 | 4798 a.u. | 1.02785 |
| 4 | 4654 a.u. | 0.99700 |
| 5 | 4664 a.u. | 0.99914 |

| | | |
|---|---|---|
| Standard Deviation (σ) | -- | 0.012823 |
| Slope (k) | -- | 0.43543 |
| Detection limit (3σ/k) | -- | 0.0883 |

**Table S8.** Sensing performance comparision between other MOF-based sensors for FA.

| *No.* | MOF-based fluorescent materials | Method | Linear range | LOD | Ref |
|---|---|---|---|---|---|
| 1 | nMOFs/Au NCs | Fluorescence | 0.15–17.5μmol/L | 0.045 μmol/L | [8] |
| 2 | *AgNPs/MIL-101(Cr)* | SERS | 0.5 –25 mmol/L | 0.3 ±0.02 nmol/L | [9] |
| 3 | $Eu_{0.06}Tb_{0.04}Gd_{0.9}$-DPNC | Fluorescence | 0-17.01μmol/L | 0.0883 μmol/L | This work |

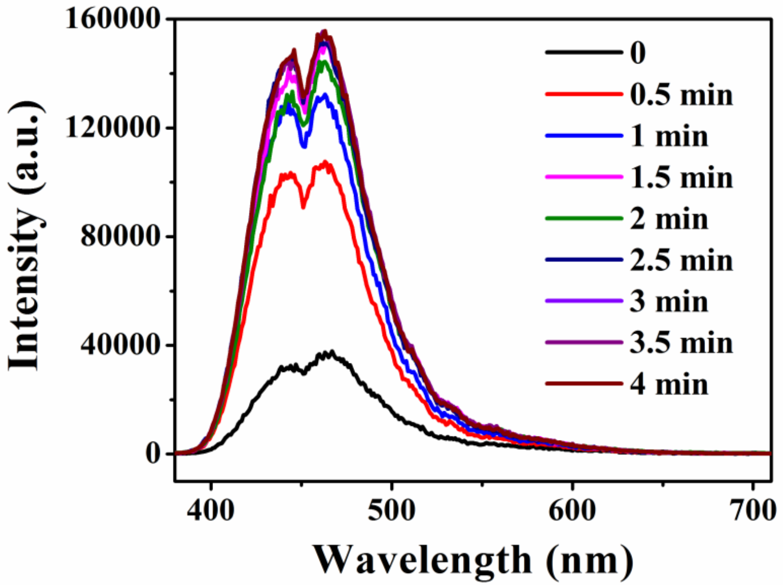


**Fig. S16.** The emission spectra of “turn-on plus” system in 0-4 minutes after the addition of FA.

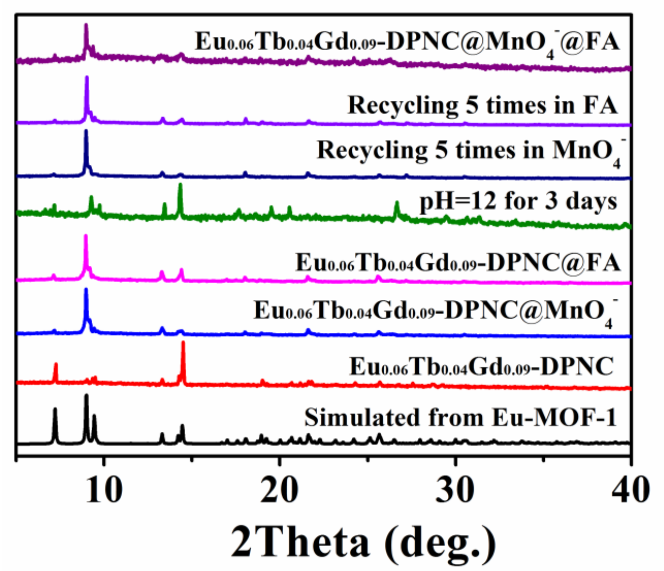


**Fig. S17.** XRD patterns of $Eu_{0.06}Tb_{0.04}Gd_{0.9}$−DPNC and after treating with different conditions.

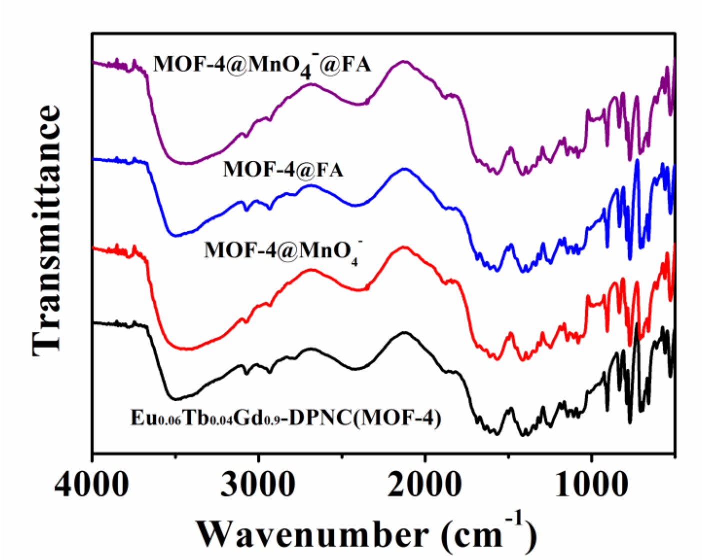


**Fig. S18.** FT-IR patterns of $Eu_{0.06}Tb_{0.04}Gd_{0.9}$−DPNC before and after soaking in $MnO_4^-$, FA and the “turn-on plus” system.

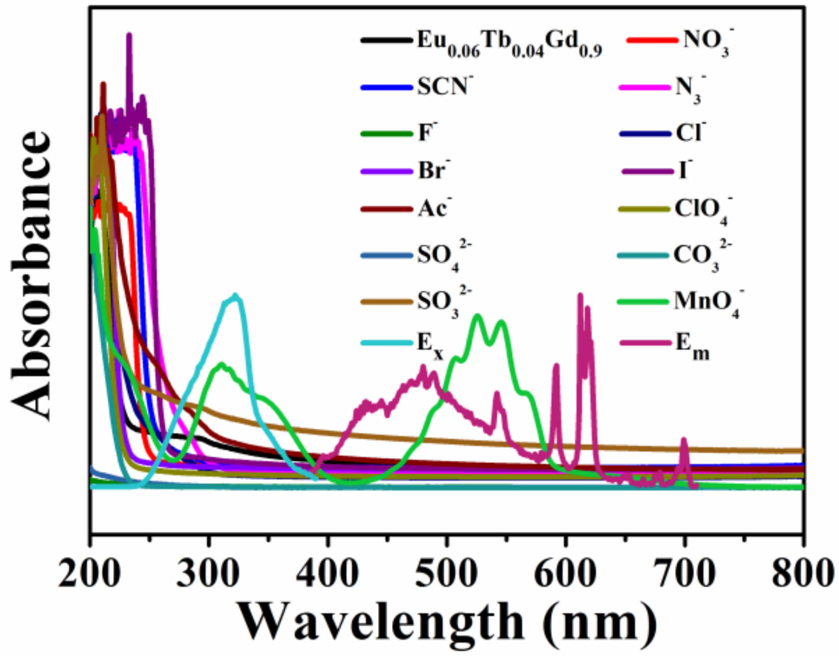


**Fig. S19.** The UV-vis spectra and excitation and emission of $Eu_{0.06}Tb_{0.04}Gd_{0.9}$–DPNC and different anionic aqueous solution.

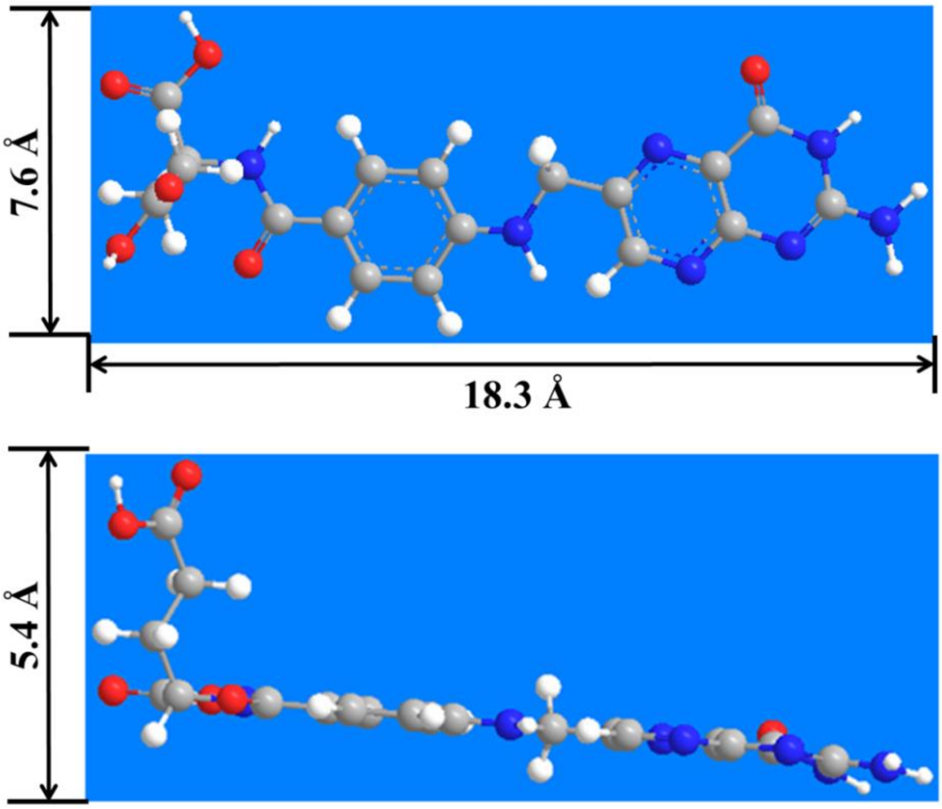


**Fig. S20.** The ball-and-stick model and the size of FA (18.3 Å × 7.6 Å × 5.4 **Å),** N, blue; C, gray; O, red; H, white**.**

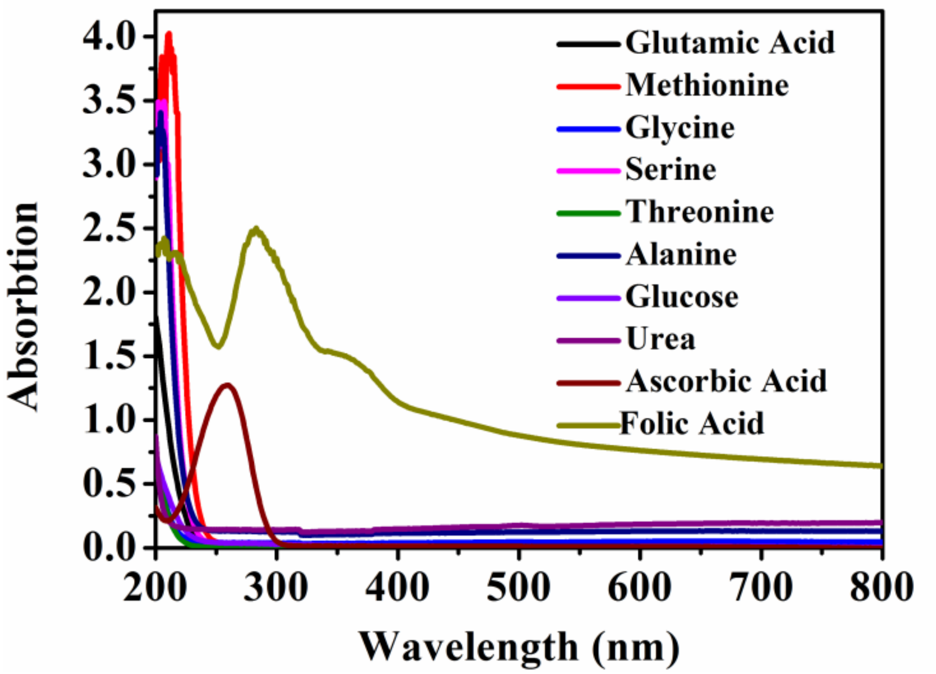


**Fig. S21.** The UV-vis spectra of different biological related substances.

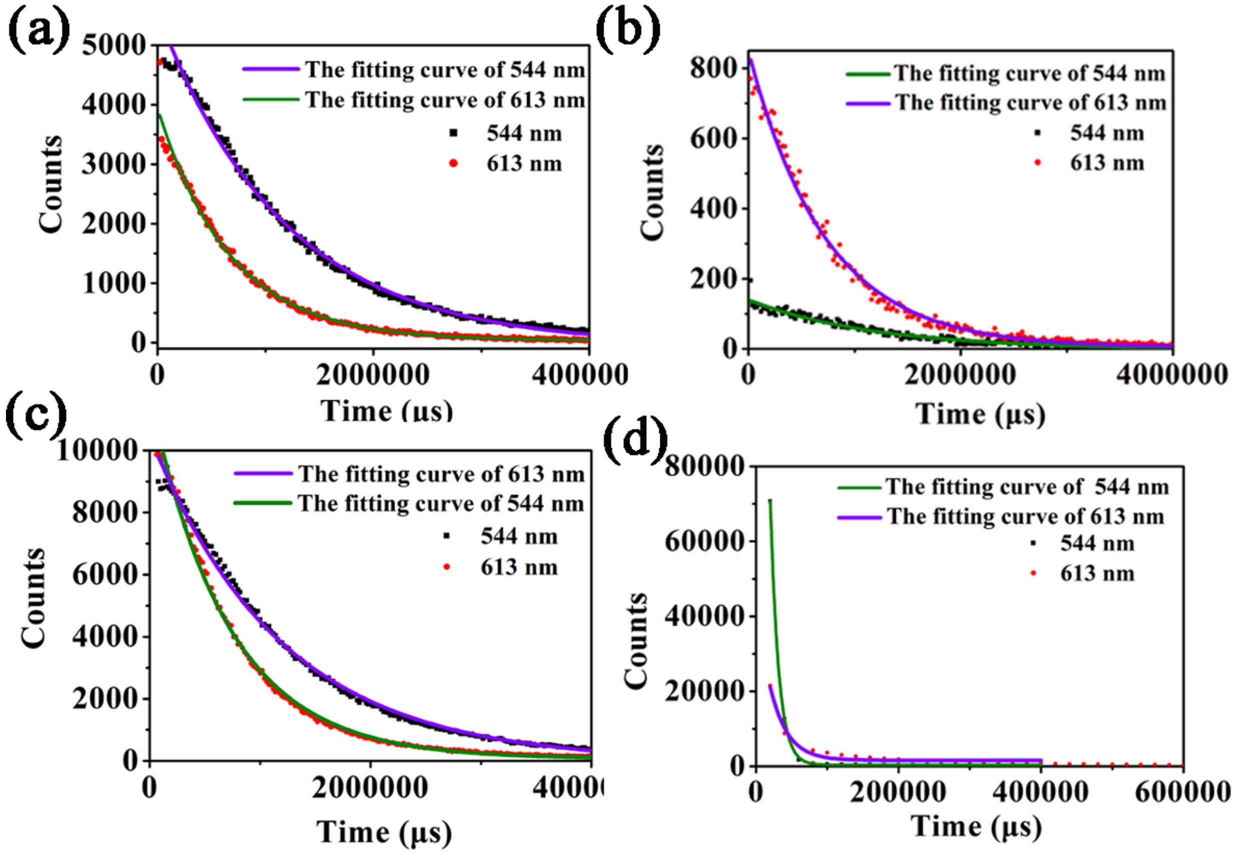


**Fig. S22.** Fluorescence decay profile of (a) $Eu_{0.06}Tb_{0.04}Gd_{0.9}$–DPNC in water, (b) $Eu_{0.06}Tb_{0.04}Gd_{0.9}$–DPNC in $MnO_4^-$ aqueous solution, (c) $Eu_{0.06}Tb_{0.04}Gd_{0.9}$–DPNC in FA aqueous solution, (d) $Eu_{0.06}Tb_{0.04}Gd_{0.9}$–DPNC in $MnO_4^-$ and FA aqueous solution excited at 365 nm.

**Table S9.** The Fluorescence lifetimes at 544 nm and 613 nm of Eu-MOF, Tb-MOF, and $Eu_{0.06}Tb_{0.04}Gd_{0.9}$–DPNC in various conditions with excitation under 365nm.

| **No.** | Fluorescence lifetime at 544 nm | Fluorescence lifetime at 613 nm |
|---|---|---|
| Eu-MOF | -- | 2.38 ms |
| Tb-MOF | 1.97 ms | -- |
| $Eu_{0.06}Tb_{0.04}Gd_{0.9}$–DPNC | 0.95 ms | 0.98 ms |
| $Eu_{0.06}Tb_{0.04}Gd_{0.9}$–DPNC in $H_2O$ | 1.17767 ms | 0.67221 ms |
| $Eu_{0.06}Tb_{0.04}Gd_{0.9}$–DPNC in $MnO_4^-$ | 1.20920 ms | 0.72989 ms |
| $Eu_{0.06}Tb_{0.04}Gd_{0.9}$–DPNC in FA | 1.18417 ms | 0.70793 ms |
| $Eu_{0.06}Tb_{0.04}Gd_{0.9}$–DPNC @$MnO_4^-$ in FA solution | 0.011346 ms | 0.024382 ms |

## Reference


[1] Nasrin Abdollahi, Ali Morsali. Highly sensitive fluorescent metal-organic framework as a selective sensor of $Mn^{VII}$ and $Cr^{VI}$ anions ($MnO_4^-/Cr_2O_7^{2-}/CrO_4^{2-}$) in aqueous solutions. Analytica Chimica Acta, 2019, 1064, 119-125.

[2] Jing-Xing Wu, Bing Yan. Eu(III)-functionalized In-MOF (In(OH)bpydc) as fluorescent probe for highly selectively sensing organic small molecules and anions especially for $CHCl_3$ and $MnO_4^-$ Journal of Colloid and Interface Science, 2017, 504, 197–205.

[3] F. Li, Y.-S. Hong, K.-X. Zuo, Q. Sun, E.-Q. Gao. Highly selective fluorescent probe for $Hg^{2+}$ and $MnO_4^-$ by the two-fold interpenetrating metal-organic framework with nitro functionalized linkers. J. Solid State Chem. 2019, 270, 509–515.

[4] M. Chen, W.-M. Xu, J.-Y. Tian, H. Cui, J.-X. Zhang, C.-S. Liu, M. Du. A terbium(III) lanthanide–organic framework as a platform for a recyclable multi-responsive luminescent sensor. J. Mater. Chem. C, 2017, 5, 2015–2021.

[5] X.-X. Zhao, Z.-B. Qin, Y.-H. Li, G.-H. Cui. Two luminescent cobalt(II) coordination polymers for selective sensing of $MnO_4^-$ in water. Transit. Metal. Chem. 2018, 43, 597 – 604.

[6] K. Wang, M. Zhu, S. Ma, X. Li, M. Zhang, E. Gao. Three water soluble coordination polymers: Synthesis, crystal structure and luminescent sensing for Cr(VI) and $MnO_4^-$ ions in the aqueous

phase. Polyhedron, 2019, 166, 60 – 64.

[7] Jun-Hua Wei, Jing-Wei Yi, Min-Le Han, Bo Li, Shan Liu, Ya-Pan Wu, Lu-Fang Ma and Dong-Sheng Li. A Water-Stable Terbium(III)–Organic Framework as a Chemosensor for Inorganic Ions, Nitro-Containing Compounds and Antibiotics in Aqueous Solutions. Chem. Asian J. 2019, 00, 0–0. (10.1002/asia.201900706)

[8] Shuguang Yan, Dongyan Deng, Lichun Zhang, Yi Lv. Fluorescence nano metal organic frameworks modulated by encapsulation for construction of versatile biosensor. Talanta, 2019, 201, 96–103.

[9] Zheng Juan Sun, Zhong Wei Jiang, Yuan Fang Li. Poly(dopamine) assisted in situ fabrication of silver nanoparticles/metal–organic framework hybrids as SERS substrates for folic acid detection. RSC Adv., 2016, 6, 79805–79810.